

**Original citation:**

LHCb Collaboration (Including: Dossett, D., Gershon, T. J., Harrison, P. F., Latham, Thomas, Poluektov, Anton, Whitehead, M. and Williams, M. P.). (2011) First observation of  $B_s \rightarrow J/\psi f_0(980)$  decays. Physics Letters B, Volume 698 (Number 2). pp. 115-122.

**Permanent WRAP url:**

<http://wrap.warwick.ac.uk/40163>

**Copyright and reuse:**

The Warwick Research Archive Portal (WRAP) makes this work of researchers of the University of Warwick available open access under the following conditions.

This article is made available under the Creative Commons Attribution- 3.0 Unported (CC BY 3.0) license and may be reused according to the conditions of the license. For more details see <http://creativecommons.org/licenses/by/3.0/>

**A note on versions:**

The version presented in WRAP is the published version, or, version of record, and may be cited as it appears here.

For more information, please contact the WRAP Team at: [publications@warwick.ac.uk](mailto:publications@warwick.ac.uk)

warwick**publications**wrap

highlight your research

<http://wrap.warwick.ac.uk/>



# First observation of $B_S^0 \rightarrow J/\psi f_0(980)$ decays <sup>☆</sup>

LHCb Collaboration

## ARTICLE INFO

**Article history:**

Received 1 February 2011  
 Received in revised form 27 February 2011  
 Accepted 1 March 2011  
 Available online 5 March 2011  
 Editor: W.-D. Schlatter

**Keywords:**

LHC  
 Hadronic  $B$  decays  
 $B_S^0$  meson

## ABSTRACT

Using data collected with the LHCb detector in proton–proton collisions at a centre-of-mass energy of 7 TeV, the hadronic decay  $B_S^0 \rightarrow J/\psi f_0(980)$  is observed. This CP eigenstate mode could be used to measure mixing-induced CP violation in the  $B_S^0$  system. Using a fit to the  $\pi^+\pi^-$  mass spectrum with interfering resonances gives  $R_{f_0/\phi} \equiv \frac{\Gamma(B_S^0 \rightarrow J/\psi f_0, f_0 \rightarrow \pi^+\pi^-)}{\Gamma(B_S^0 \rightarrow J/\psi \phi, \phi \rightarrow K^+K^-)} = 0.252^{+0.046+0.027}_{-0.032-0.033}$ . In the interval  $\pm 90$  MeV around 980 MeV, corresponding to approximately two full  $f_0$  widths we also find  $R' \equiv \frac{\Gamma(B_S^0 \rightarrow J/\psi \pi^+\pi^-, |m(\pi^+\pi^-) - 980 \text{ MeV}| < 90 \text{ MeV})}{\Gamma(B_S^0 \rightarrow J/\psi \phi, \phi \rightarrow K^+K^-)} = 0.162 \pm 0.022 \pm 0.016$ , where in both cases the uncertainties are statistical and systematic, respectively.

© 2011 CERN. Published by Elsevier B.V. All rights reserved.

## 1. Introduction

In  $B_S^0$  decays some final states can be reached either by a direct decay amplitude or via a mixing amplitude. For the case of  $B_S^0 \rightarrow J/\psi \phi$  decays, the interference between these two amplitudes allows observation of a CP violating phase. In the Standard Model (SM) this phase is  $-2\beta_s = -0.036^{+0.0020}_{-0.0016}$  radians, where  $\beta_s = \arg(-V_{ts}V_{tb}^*/V_{cs}V_{cb}^*)$ , and the  $V_{ij}$  are CKM matrix elements [1]. This is about 20 times smaller in magnitude than the measured value of the corresponding phase  $2\beta$  in  $B^0$  mixing. Being small, this phase can be drastically increased by the presence of new particles beyond the SM. Thus, measuring  $\beta_s$  is an important probe of new physics.

Attempts to determine  $\beta_s$  have been made by the CDF and D0 experiments at the Tevatron using the  $B_S^0 \rightarrow J/\psi \phi$  decay mode [2]. While initial results hinted at possible large deviations from the SM, recent measurements are more consistent [3,4]. However, the Tevatron limits are still not very constraining. Since the final state consists of two spin-1 particles, it is not a CP eigenstate. While it is well known that CP violation can be measured using angular analyses [5], this requires more events to gain similar sensitivities to those obtained if the decay proceeds via only CP-even or CP-odd channels. In Ref. [6] it is argued that in the case of  $J/\psi \phi$  the analysis is complicated by the presence of an S-wave  $K^+K^-$  system interfering with the  $\phi$  that must be taken into account, and that this S-wave would also manifest itself by the appearance of  $f_0(980) \rightarrow \pi^+\pi^-$  decays. This decay  $B_S^0 \rightarrow J/\psi f_0(980)$  is to a single CP-odd eigenstate and does not require an angular analysis. Its CP violating phase in the Standard Model is  $-2\beta_s$  (up to correc-

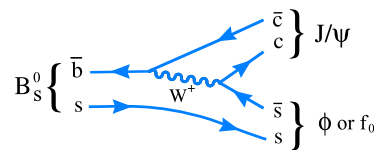


Fig. 1. Decay diagram for  $B_S^0 \rightarrow J/\psi (f_0 \text{ or } \phi)$  decays.

tions due to higher order diagrams). In what follows, we use the notation  $f_0$  to refer to the  $f_0(980)$  state.

By comparing  $D_s^+ \rightarrow f_0 \pi^+$  decays where the  $f_0$  was detected in both  $K^+K^-$  and  $\pi^+\pi^-$  modes it was predicted that [6]

$$R_{f_0/\phi} \equiv \frac{\Gamma(B_S^0 \rightarrow J/\psi f_0, f_0 \rightarrow \pi^+\pi^-)}{\Gamma(B_S^0 \rightarrow J/\psi \phi, \phi \rightarrow K^+K^-)} \approx 20\%. \quad (1)$$

A decay rate at this level would make these events very useful for measuring  $\beta_s$  if backgrounds are not too large.

The dominant decay diagram for these processes is shown in Fig. 1. It is important to realize that the  $s\bar{s}$  system accompanying the  $J/\psi$  is an isospin singlet (isoscalar), and thus cannot produce a single meson that is anything but isospin zero. Thus, for example, in this spectator model production of a  $\rho^0$  meson is forbidden. The dominant low mass isoscalar resonance decaying into  $\pi^+\pi^-$  is the  $f_0(980)$  but other higher mass objects are possible.

Although the  $f_0$  mass is relatively well estimated at  $980 \pm 10$  MeV (we use units with  $c = 1$ ) by the PDG, the width is poorly known. Its measurement appears to depend on the final state, and is complicated by the opening of the  $KK$  channel close to the pole; the PDG estimates 40–100 MeV [11]. Recently CLEO measured these properties in the semileptonic decay  $D_s^+ \rightarrow f_0 e^+ \nu$ , where hadronic effects are greatly reduced, determining a width of  $(91^{+30}_{-22} \pm 3)$  MeV [12].

<sup>☆</sup> © CERN, for the benefit of the LHCb Collaboration.

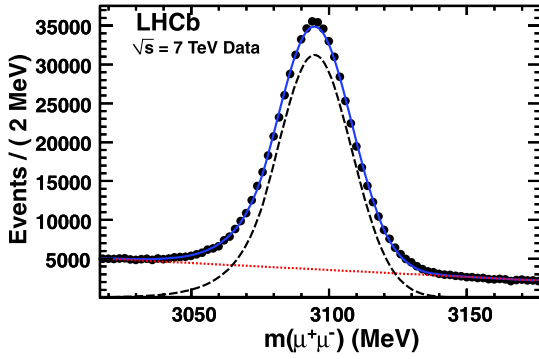


Fig. 2. The  $\mu^+\mu^-$  invariant mass for candidates satisfying the trigger and analysis requirements and having  $t_z > 0.5$  ps. The data points are shown as circles; the error bars are smaller than the circle radii. The dashed line shows the Crystal Ball signal function [10], the dotted line the background and the solid line the sum.

## 2. Data sample and analysis requirements

We use a data sample of approximately  $33 \text{ pb}^{-1}$  collected with the LHCb detector in 2010 [7]. The detector elements are placed along the beam line of the LHC starting with the Vertex Locator (VELO), a silicon strip device that surrounds the proton–proton interaction region and is positioned 8 mm from the beam during collisions. It provides precise locations for primary  $pp$  interaction vertices, the locations of decays of long-lived particles, and contributes to the measurement of track momenta. Other devices used to measure track momenta comprise a large area silicon strip detector (TT) located in front of a 3.7 Tm dipole magnet, and a combination of silicon strip detectors (IT) and straw drift chambers (OT) placed behind. Two Ring Imaging Cherenkov (RICH) detectors are used to identify charged hadrons. Further downstream an Electromagnetic Calorimeter (ECAL) is used for photon detection and electron identification, followed by a Hadron Calorimeter (HCAL), and a system consisting of alternating layers of iron and chambers (MWPC and triple-GEM) that distinguishes muons from hadrons (MUON). The ECAL, MUON, and HCAL provide the capability of first-level hardware triggering.

This analysis is restricted to events accepted by a  $J/\psi \rightarrow \mu^+\mu^-$  trigger. Subsequent analysis selection criteria are applied that serve to reject background, yet preserve high efficiencies on both the  $J/\psi\pi^+\pi^-$  and  $J/\psi K^+K^-$  final states, as determined by Monte Carlo events generated using PYTHIA [8], and LHCb detector simulation based on GEANT4 [9]. Tracks are reconstructed as described in Ref. [7]. To be considered as a  $J/\psi \rightarrow \mu^+\mu^-$  candidate opposite sign tracks are required to have transverse momentum,  $p_T$ , greater than 500 MeV, be identified as muons, and form a common vertex with fit  $\chi^2$  per number of degrees of freedom (ndof) less than 11. The  $\mu^+\mu^-$  invariant mass distribution is shown in Fig. 2 with an additional requirement, used only for this plot, that the pseudo proper-time,  $t_z$ , be greater than 0.5 ps, where  $t_z$  is the distance that the  $J/\psi$  candidate travels downstream parallel to the beam, along  $z$ , times the known  $J/\psi$  mass divided by the  $z$  component of the candidate’s momentum. The data are fit with a Crystal Ball signal function [10] to account for the radiative tail towards low mass, and a linear background function. There are  $549,000 \pm 1100 J/\psi$  signal events in the entire mass range. For subsequent use only candidates within  $\pm 48$  MeV of the known  $J/\psi$  mass are selected.

Pion and kaon candidates are selected if they are inconsistent with having been produced at the closest primary vertex. The impact parameter (IP) is the minimum distance of approach of the track with respect to the primary vertex. We require that the  $\chi^2$  formed by using the hypothesis that the IP is equal to zero be  $> 9$

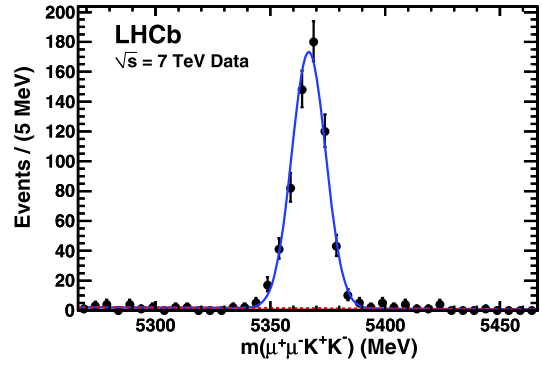


Fig. 3. The invariant mass of  $J/\psi K^+K^-$  combinations when the  $K^+K^-$  pair is required to be with  $\pm 20$  MeV of the  $\phi$  mass. The data have been fit with a Gaussian signal function whose mass and width are allowed to float and linear background function shown as a dashed line. The solid curve shows the sum.

for each track. For further consideration these tracks must be positively identified in the RICH system. Particles forming opposite-sign di-pion candidates must have their scalar sum  $p_T > 900$  MeV, while those forming opposite-sign di-kaon candidates must have their vector sum  $p_T > 1000$  MeV, and have an invariant mass within  $\pm 20$  MeV of the  $\phi$  mass.

To select  $B_s^0$  candidates we further require that the two pions or kaons form a vertex with a  $\chi^2 < 10$ , that they form a candidate  $B_s^0$  vertex with the  $J/\psi$  where the vertex fit  $\chi^2/\text{ndof} < 5$ , and that this  $B_s^0$  candidate points to the primary vertex at an angle not different from its momentum direction by more than  $0.68^\circ$ .

Simulations are used to evaluate our detection efficiencies. For the  $J/\psi\phi$  final state we use the measured decay parameters from CDF [3]. The  $J/\psi f_0$  final state is simulated using full longitudinal polarization of the  $J/\psi$  meson. The efficiencies of having all four decay tracks in the geometric acceptance and satisfying the trigger, track reconstruction and data selection requirements are  $(1.471 \pm 0.024)\%$  for  $J/\psi f_0$ , requiring the  $\pi^+\pi^-$  invariant mass be within  $\pm 500$  MeV of 980 MeV, and  $(1.454 \pm 0.021)\%$  for  $J/\psi\phi$ , having the  $K^+K^-$  invariant mass be within  $\pm 20$  MeV of the  $\phi$  mass. The uncertainties on the efficiency estimates are statistical only.

## 3. Results

The  $J/\psi K^+K^-$  invariant mass distribution is shown in Fig. 3. The di-muon invariant mass has been constrained to have the known value of the  $J/\psi$  mass; this is done for all subsequent  $B_s^0$  invariant mass distributions. The data are fit with a Gaussian signal function and a linear background function. The fit gives a  $B_s^0$  mass of  $5366.7 \pm 0.4$  MeV, a width of 7.4 MeV r.m.s., and a yield of  $635 \pm 26$  events.

Initially, to search for a  $f_0(980)$  signal we restrict ourselves to an interval of  $\pm 90$  MeV around the  $f_0$  mass, approximately two full  $f_0$  widths [12]. The  $B_s^0$  candidate invariant mass distribution for selected  $J/\psi\pi^+\pi^-$  combinations is shown in Fig. 4. The signal is fit with a Gaussian whose mean and width are allowed to float. We also include a background component due to  $B^0 \rightarrow J/\psi\pi^+\pi^-$  that is taken to be Gaussian, with mass allowed to float in the fit, but whose width is constrained to be the same as the  $B_s^0$  signal. Other components in the fit are  $B^0 \rightarrow J/\psi K^{*0}$ , combinatorial background taken to have an exponential shape,  $B^+ \rightarrow J/\psi K^+$  (or  $\pi^+$ ), and other specific  $B_s^0$  decay backgrounds including  $B_s^0 \rightarrow J/\psi\eta'$ ,  $\eta' \rightarrow \rho\gamma$ ,  $B_s^0 \rightarrow J/\psi\phi$ ,  $\phi \rightarrow \pi^+\pi^-\pi^0$ . The shape of the sum of the combinatorial and  $B^+ \rightarrow J/\psi K^+$  ( $\pi^+$ ) components is taken from the like-sign events. The shapes of the other components are taken from Monte Carlo simulation with their normalizations allowed to float.

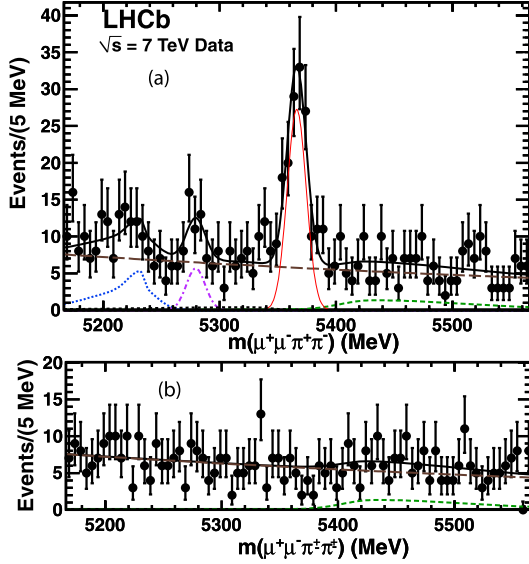


**Fig. 4.** (a) The invariant mass of  $J/\psi\pi^+\pi^-$  combinations when the  $\pi^+\pi^-$  pair is required to be with  $\pm 90$  MeV of the  $f_0(980)$  mass. The data have been fit with a signal Gaussian and several background functions. The thin (red) solid curve shows the signal, the long-dashed (brown) curve the combinatorial background, the dashed (green) curve the  $B^+ \rightarrow J/\psi K^+(\pi^+)$  background, the dotted (blue) curve the  $B^0 \rightarrow J/\psi K^{*0}$  background, the dash-dot curve (purple) the  $B^0 \rightarrow J/\psi\pi^+\pi^-$  background, the barely visible dotted curve (black) the sum of  $B^0 \rightarrow J/\psi\eta'$  and  $J/\psi\phi$  backgrounds, and the thick-solid (black) curve the total. (b) The same as above but for like-sign di-pion combinations. (For interpretation of the references to color in this figure legend, the reader is referred to the web version of this Letter.)

We perform a simultaneous unbinned likelihood fit to the  $\pi^+\pi^-$  opposite-sign and sum of  $\pi^+\pi^+$  and  $\pi^-\pi^-$  like-sign event distributions. The fit gives a  $B_s^0$  mass of  $5366.1 \pm 1.1$  MeV in good agreement with the known mass of  $5366.3 \pm 0.6$  MeV, a Gaussian width of  $8.2 \pm 1.1$  MeV, consistent with the expected mass resolution and  $111 \pm 14$  signal events within  $\pm 30$  MeV of the  $B_s^0$  mass. The change in twice the natural logarithm of the fit likelihood when removing the  $B_s^0$  signal component, shows that the signal has an equivalent of 12.8 standard deviations of significance. The like-sign di-pion yield correctly describes the shape and level of the background below the  $B_s^0$  signal peak, both in data and Monte Carlo simulations. There are also  $23 \pm 9$   $B^0 \rightarrow J/\psi\pi^+\pi^-$  events.

Having established a clear signal, we perform certain checks to ascertain if the structure peaking near 980 MeV is a spin-0 object. Since the  $B_s^0$  is spinless, when it decays into a spin-1  $J/\psi$  and a spin-0  $f_0$ , the decay angle of the  $J/\psi$  should be distributed as  $1 - \cos^2\theta_{J/\psi}$ , where  $\theta_{J/\psi}$  is the angle of the  $\mu^+$  in the  $J/\psi$  rest frame with respect to the  $B_s^0$  direction. The polarization angle,  $\theta_{f_0}$ , the angle of the  $\pi^+$  in the  $f_0$  rest frame with respect to the  $B_s^0$  direction, should be uniformly distributed. A simulation of the  $J/\psi$  detection efficiency in these decays shows that it is approximately independent of  $\cos\theta_{J/\psi}$ . The acceptance for  $f_0 \rightarrow \pi^+\pi^-$  as a function of the  $\pi^+$  decay angle shows an inefficiency of about 50% at  $\cos\theta_{f_0} = \pm 1$  with respect to its value at  $\cos\theta_{f_0} = 0$ . It is fit to a parabola and the inefficiency corrected in what follows.

The like-sign background subtracted  $J/\psi$  helicity distribution is fit to a  $1 - \alpha \cos^2\theta_{J/\psi}$  function as shown in Fig. 5(a). The fit gives  $\alpha = 0.81 \pm 0.21$  consistent with a longitudinally polarized  $J/\psi$  (spin perpendicular to its momentum) and a spin-0  $f_0$  meson. The  $\chi^2$  of the fit is 10.3 for 8 degrees of freedom. Similarly, we subtract the like-sign background and fit the efficiency corrected  $\pi^+\pi^-$  helicity distribution to a constant function as shown

in Fig. 5(b). The fit has a  $\chi^2/\text{ndof}$  equal to 15.9/9, still consistent with a uniform distribution as expected for a spinless particle.

To view the spectrum of  $\pi^+\pi^-$  masses, between 580 and 1480 MeV, in the  $J/\psi\pi^+\pi^-$  final state we select events within  $\pm 30$  MeV of the  $B_s^0$  and plot the invariant mass spectrum in Fig. 6. The data show a strong peak near 980 MeV and an excess of events above the like-sign background extending up to 1500 MeV. Our mass spectrum is similar in shape to those seen previously in studies of the S-wave  $\pi^+\pi^-$  system with  $s\bar{s}$  quarks in the initial state [13–15]. To establish a value for  $R_{f_0/\phi}$  requires fitting the shape of the  $f_0$  resonance. Simulation shows that our acceptance is independent of the  $\pi^+\pi^-$  mass, and we choose an interval between 580 and 1480 MeV. Guidance is given by the BES Collaboration who fit the spectrum in  $J/\psi \rightarrow \phi\pi^+\pi^-$  decays [14]. We include here the  $f_0(980)$  and  $f_0(1370)$  resonances, though other final states may be present, for example the  $f_2(1270)$  a  $2^{++}$  state [13,14]; it will take much larger statistics to sort out the higher mass states. We use a coupled-channel Breit-Wigner amplitude (Flatté) for the  $f_0(980)$  resonance [16] and a Breit-Wigner shape (BW) for the higher mass  $f_0(1370)$ . Defining  $m$  as the  $\pi^+\pi^-$  invariant mass, the mass distribution is fit with a function involving the square of the interfering amplitudes

$$|A(m)|^2 = N_0 m p(m) q(m) |\text{Flatté}[f_0(980)] + A_1 \exp^{(i\delta)} \text{BW}[f_0(1370)]|^2, \quad (2)$$

where  $N_0$  is a normalization constant,  $p(m)$  is the momentum of the  $\pi^+$ ,  $q(m)$  the momentum of the  $J/\psi$  in the  $\pi^+\pi^-$  rest-frame, and  $\delta$  is the relative phase between the two components. The Flatté amplitude is defined as

$$\text{Flatté}(m) = \frac{1}{m_0^2 - m^2 - im_0(g_1\rho_{\pi\pi} + g_2\rho_{KK})}, \quad (3)$$

where  $m_0$  refers to the mass of the  $f_0(980)$  and  $\rho_{\pi\pi}$  and  $\rho_{KK}$  are Lorentz invariant phase space factors equal to  $2p(m)/m$  for  $\rho_{\pi\pi}$ . The  $g_2\rho_{KK}$  term accounts for the opening of the kaon threshold. Here  $\rho_{KK} = 2p_K(m)/m$  where  $p_K(m)$  is the momentum a kaon would have in the  $\pi^+\pi^-$  rest-frame. It is taken as an imaginary number when  $m$  is less than twice the kaon mass. We use  $m_0g_1 = 0.165 \pm 0.018$  GeV<sup>2</sup>, and  $g_2/g_1 = 4.21 \pm 0.33$  as determined by BES [14].

The  $f_0(1370)$  mass and width values used here are  $1434 \pm 20$  MeV, and  $172 \pm 33$  MeV from an analysis by E791 [15]. We fix the central values of these masses and widths in the fit, as well as  $m_0g_1$  and the  $g_2/g_1$  ratio for the  $f_0(980)$  amplitude. The mass resolution is incorporated as a Gaussian convolution in the fit as a function of  $\pi^+\pi^-$  mass. It has an r.m.s. of 5.4 MeV at 980 MeV. We fit both the opposite-sign and like-sign distributions simultaneously. The results of the fit are shown in Fig. 6. The  $\chi^2/\text{ndof}$  is 44/56. We find an  $f_0(980)$  mass value of  $972 \pm 25$  MeV. There are  $265 \pm 26$  events above background in the extended mass region, of which  $(64_{-6}^{+10})\%$  are associated with the  $f_0(980)$ ,  $(12 \pm 4)\%$  are ascribed to the  $f_0(1370)$  and  $(24_{-6}^{+2})\%$  are from interference. The fit determines  $\delta = 61 \pm 36^\circ$ . The fit fraction is defined as the integral of a single component divided by the coherent sum of all components. The  $f_0(980)$  yield is  $169_{-21}^{+31}$  events. The lower mass cutoff of the fit region loses 1% of the  $f_0(980)$  events. The change in twice the log likelihood of the fit when removing the  $f_0(980)$  component shows that it has an equivalent of 12.5 standard deviations of significance.

Using the 169  $f_0$  events from  $J/\psi\pi^+\pi^-$ , and the 635  $\phi$  events from  $J/\psi K^+K^-$ , correcting by the relative efficiency, and ignor-

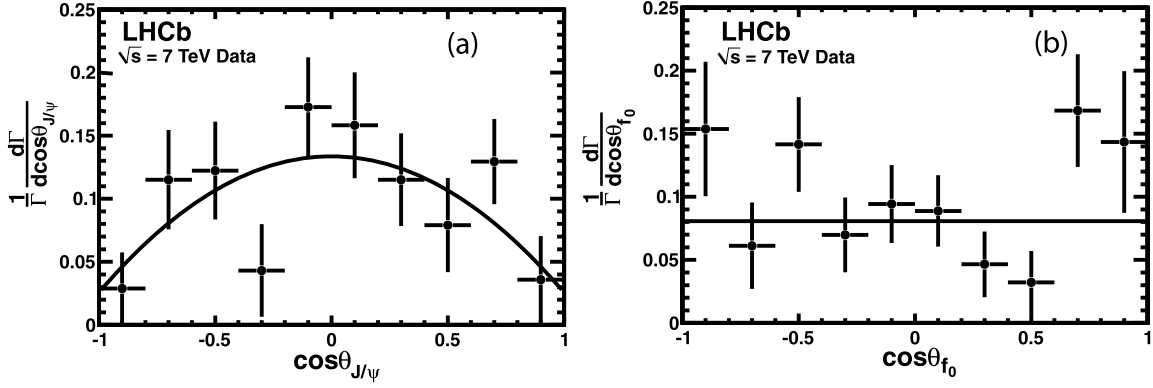


**Fig. 5.** Angular distributions of events within  $\pm 30$  MeV of the  $B_s^0$  mass and  $\pm 90$  MeV of the  $f_0$  mass after like-sign background subtraction. (a) The cosine of the angle of the  $\mu^+$  with respect to the  $B_s^0$  direction in the  $J/\psi$  rest frame for  $B_s^0 \rightarrow J/\psi \pi^+ \pi^-$  decays. The data are fit with a function  $f(\cos \theta_{J/\psi}) = 1 - \alpha \cos^2 \theta_{J/\psi}$ . (b) The cosine of the angle of the  $\pi^+$  with respect to the  $B_s^0$  direction in the di-pion rest frame for  $B_s^0 \rightarrow J/\psi \pi^+ \pi^-$  decays. The data are fit with a flat line.

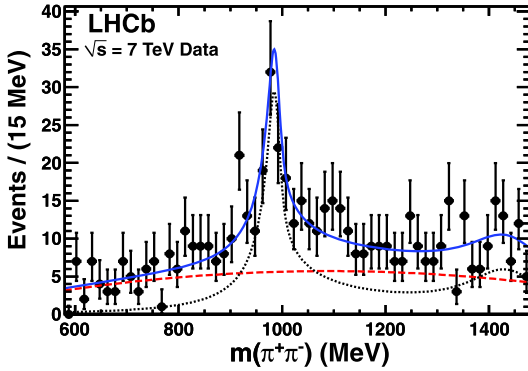


**Fig. 6.** The invariant mass of  $\pi^+ \pi^-$  combinations when the  $J/\psi \pi^+ \pi^-$  is required to be within  $\pm 30$  MeV of the  $B_s^0$  mass. The dashed curve is the like-sign background that is taken from the data both in shape and absolute normalization. The dotted curve is the result of the fit using Eq. (2) and the solid curve the total.

ing a possible small S-wave contribution under the  $\phi$  peak [17], yields

$$R_{f_0/\phi} \equiv \frac{\Gamma(B_s^0 \rightarrow J/\psi f_0, f_0 \rightarrow \pi^+ \pi^-)}{\Gamma(B_s^0 \rightarrow J/\psi \phi, \phi \rightarrow K^+ K^-)} = 0.252^{+0.046+0.027}_{-0.032-0.033}. \quad (4)$$

Here and throughout this Letter whenever two uncertainties are quoted the first is statistical and the second is systematic. This value of  $R_{f_0/\phi}$  depends on the decay amplitudes used to fit the  $\pi^+ \pi^-$  mass distribution and could change with different assumptions. To check the robustness of this result, an incoherent phase space background is added to the above fit function. The number of signal  $f_0(980)$  events is decreased by 7.3%. If we leave the  $f_0(1370)$  out of this fit, the original  $f_0(980)$  yield is decreased by 6.5%. The larger number of these two numbers is included in the systematic uncertainty. The BES Collaboration also included a  $\sigma$  resonance in their fit to the  $\pi^+ \pi^-$  mass spectrum in  $J/\psi \rightarrow \phi \pi^+ \pi^-$  decays [14]. We do not find it necessary to add this component to the fit.

The systematic uncertainty has several contributions listed in Table 1. There is an uncertainty due to our kaon and pion identification. The identification efficiency is measured with respect to the Monte Carlo simulation using samples of  $D^{*+} \rightarrow \pi^+ D^0$ ,  $D^0 \rightarrow K^- \pi^+$  events for kaons, and samples of  $K_S^0 \rightarrow \pi^+ \pi^-$  decays for pions. The correction to  $R_{f_0/\phi}$  is  $0.947 \pm 0.009$ . This correction is already included in the efficiencies quoted above, and

**Table 1**

Relative systematic uncertainties on  $R_{f_0/\phi}$  (%). Both negative and positive changes resulting from the parameter variations are indicated in separate columns.

Parameter	Negative change	Positive change
$f_0(1370)$ mass	0.3	1.9
$f_0(1370)$ width	2.3	2.6
$\pi^+ \pi^-$ mass dependent efficiency	2.3	2.3
$m_0 g_1$	4.2	3.6
$g_2/g_1$	0.7	0.7
Addition of non-resonant $\pi^+ \pi^-$	7.3	0
MC statistics (efficiency ratio)	2.3	2.3
$B_s^0 p_T$ distribution	0.5	0.5
$B_s^0$ mass resolution	0.5	0.5
PID efficiency	1.0	1.0
$\phi$ detection	9.0	9.0
Total	13.1	10.8

the 1% systematic uncertainty is assigned for the relative particle identification efficiencies.

The efficiency for detecting  $\phi \rightarrow K^+ K^-$  versus a  $\pi^+ \pi^-$  pair is measured using  $D^+$  meson decays into  $\phi \pi^+$  and  $K^- \pi^+ \pi^+$  in a sample of semileptonic  $B$  decays where  $B \rightarrow D^+ X \mu^- \bar{\nu}$  [18]. The simulation underestimates the  $\phi$  efficiency relative to the  $\pi^+ \pi^-$  efficiency by  $(6 \pm 9)\%$ , so we take 9% as the systematic error.

Besides the sources of uncertainty discussed above, there is a variation due to varying the parameters of the two resonant contributions. We also include an uncertainty for a mass dependent efficiency as a function of  $\pi^+ \pi^-$  mass by changing the acceptance function from flat to linear and found that the  $f_0$  yield changed by 2.3%. The difference  $\Delta\Gamma/\Gamma$  between CP-even and CP-odd  $B_s$  eigenstates is taken as 0.088.

In order to give a model independent result we also quote the fraction,  $R'$ , in the interval  $\pm 90$  MeV around 980 MeV, corresponding to approximately two full-widths, where there are  $111 \pm 14$  events. Then

$$R' \equiv \frac{\Gamma(B_s^0 \rightarrow J/\psi \pi^+ \pi^-, |m(\pi^+ \pi^-) - 980 \text{ MeV}| < 90 \text{ MeV})}{\Gamma(B_s^0 \rightarrow J/\psi \phi, \phi \rightarrow K^+ K^-)} = 0.162 \pm 0.022 \pm 0.016. \quad (5)$$

This ratio is based on the fit to the  $B_s^0$  mass distribution and does not have any uncertainties related to the fit of the  $\pi^+ \pi^-$  mass distribution. Based on our fits to the  $\pi^+ \pi^-$  mass distribution, there are negligible contributions from any other signal components than the  $f_0(980)$  in this interval.

The original estimate from Stone and Zhang was  $R_{f_0/\phi} = 0.20$  [6]. More recent predictions have been summarized by Stone [19] and have a rather wide range from 0.07 to 0.50.



#### 4. Conclusions

Based on the polarization and rate estimates described above, the first observation of a new CP-odd eigenstate decay mode of the  $B_s^0$  meson into  $J/\psi f_0(980)$  has been made. Using a fit including two interfering resonances, the  $f_0(980)$  and  $f_0(1370)$ , the ratio to  $J/\psi\phi$  production is measured as

$$R_{f_0/\phi} \equiv \frac{\Gamma(B_s^0 \rightarrow J/\psi f_0, f_0 \rightarrow \pi^+\pi^-)}{\Gamma(B_s^0 \rightarrow J/\psi\phi, \phi \rightarrow K^+K^-)} = 0.252_{-0.032-0.033}^{+0.046+0.027}. \quad (6)$$

By selecting events within  $\pm 90$  MeV of the  $f_0(980)$  mass the ratio becomes  $R' = 0.162 \pm 0.022 \pm 0.016$ .

The events around the  $f_0(980)$  mass are large enough in rate and have small enough backgrounds that they could be used to measure  $\beta_s$  without angular analysis. It may also be possible to use other data in the  $\pi^+\pi^-$  mass region above the  $f_0(980)$  for this purpose if they turn out to be dominated by S-wave.

#### Acknowledgements

We express our gratitude to our colleagues in the CERN accelerator departments for the excellent performance of the LHC. We thank the technical and administrative staff at CERN and at the LHCb institutes, and acknowledge support from the National Agencies: CAPES, CNPq, FAPERJ and FINEP (Brazil); CERN; NSFC (China); CNRS/IN2P3 (France); BMBF, DFG, HGF and MPG (Germany); SFI (Ireland); INFN (Italy); FOM and NWO (Netherlands); SCSR (Poland); ANCS (Romania); MinES of Russia and Rosatom (Russia); MICINN, XUNGAL and GENCAT (Spain); SNSF and SER (Switzerland); NAS Ukraine (Ukraine); STFC (United Kingdom); NSF (USA). We also acknowledge the support received from the ERC under FP7 and the Région Auvergne.

#### Open access

This article is published Open Access at [sciencedirect.com](http://sciencedirect.com). It is distributed under the terms of the Creative Commons Attribution License 3.0, which permits unrestricted use, distribution, and reproduction in any medium, provided the original authors and source are credited.

tion License 3.0, which permits unrestricted use, distribution, and reproduction in any medium, provided the original authors and source are credited.

#### References

- [1] J. Charles, et al., Eur. Phys. J. C 41 (2005) 1.
- [2] T. Aaltonen, et al., CDF Collaboration, Phys. Rev. Lett. 100 (2008) 121803; V.M. Abazov, et al., D0 Collaboration, Phys. Rev. Lett. 101 (2008) 241801.
- [3] G. Giurgiu, for the CDF Collaboration, arXiv:1012.0962 [hep-ex], Proc. of 35th Int. Conf. of High Energy Physics, July 2010, Paris, France, in press.
- [4] R. Van Kooten, CP violation studies in the  $B_s^0$  system at D0, presented at the 35th Int. Conf. of High Energy Physics, July 2010, Paris, France.
- [5] I. Dunietz, H.R. Quinn, A. Snyder, W. Toki, H.J. Lipkin, Phys. Rev. D 43 (1991) 2193; J.L. Rosner, Phys. Rev. D 42 (1990) 3732; A.S. Dighe, I. Dunietz, H.J. Lipkin, J.L. Rosner, Phys. Lett. B 369 (1996) 144.
- [6] S. Stone, L. Zhang, Phys. Rev. D 79 (2009) 074024.
- [7] A. Augusto Alves Jr., et al., LHCb Collaboration, JINST 3 (2008) S08005.
- [8] T. Sjöstrand, S. Mrenna, P. Skands, JHEP 0605 (2006) 026.
- [9] S. Agostinelli, et al., Nucl. Instrum. and Meth. 506 (2003) 250.
- [10] J.E. Gaiser, PhD thesis, SLAC-R-255 (1982), Appendix F; T. Skwarnicki, PhD thesis, DESY F31-86-02 (1986), Appendix E.
- [11] K. Nakamura, et al., Particle Data Group, J. Phys. G 37 (2010) 075021.
- [12] K.M. Ecklund, et al., CLEO Collaboration, Phys. Rev. D 80 (2009) 052009.
- [13] B. Aubert, et al., BaBar Collaboration, Phys. Rev. D 79 (2009) 032003.
- [14] M. Ablikim, et al., BES Collaboration, Phys. Lett. B 607 (2005) 243.
- [15] E.M. Aitala, et al., E791 Collaboration, Phys. Rev. Lett. 86 (2001) 765.
- [16] S.M. Flatté, Phys. Lett. B 63 (1976) 224.
- [17] The CDF Collaboration limits the S-wave contribution within  $\pm 10$  MeV of the  $\phi$  mass to 6.7% at 95% confidence level. Their best fit value is 2% [3].
- [18] We measure the  $K^+K^-\pi^+$  yield from  $D^+$  decays. Then the  $\phi$  yield is extracted and compared with the  $0.28 \pm 0.05$  measured fraction of  $K^+K^-$  within 20 MeV of the  $\phi$  mass from the CLEO-c Dalitz analysis. See P. Rubin, et al., CLEO Collaboration, Phys. Rev. D 78 (2008) 072003. Finally we use the measured branching fraction ratio of  $K^+K^-\pi^+/K^+\pi^-\pi^+$  in  $D^+$  decays of  $(10.58 \pm 0.29)\%$  [11] to compare with Monte Carlo simulation.
- [19] S. Stone, arXiv:1009.4939 [hep-ph], Proc. of Flavor Physics and CP Violation 2010, May 2010, Torino, Italy, in press; See also: P. Colangelo, F. De Fazio, W. Wang, Phys. Rev. D 81 (2010) 074001; P. Colangelo, F. De Fazio, W. Wang, arXiv:1009.4612 [hep-ph]; O. Leitner, et al., Phys. Rev. D 82 (2010) 076006.

#### LHCb Collaboration

R. Aaij<sup>23</sup>, B. Adeva<sup>36</sup>, M. Adinolfi<sup>42</sup>, C. Adrover<sup>6</sup>, A. Affolder<sup>48</sup>, Z. Ajaltouni<sup>5</sup>, J. Albrecht<sup>37</sup>, F. Alessio<sup>6,37</sup>, M. Alexander<sup>47</sup>, P. Alvarez Cartelle<sup>36</sup>, A.A. Alves Jr.<sup>22</sup>, S. Amato<sup>2</sup>, Y. Amhis<sup>38</sup>, J. Amoraal<sup>23</sup>, J. Anderson<sup>39</sup>, R.B. Appleby<sup>50</sup>, O. Aquines Gutierrez<sup>10</sup>, L. Arrabito<sup>53</sup>, M. Artuso<sup>52</sup>, E. Aslanides<sup>6</sup>, G. Aurieremma<sup>22,m</sup>, S. Bachmann<sup>11</sup>, D.S. Bailey<sup>50</sup>, V. Balagura<sup>30,37</sup>, W. Baldini<sup>16</sup>, R.J. Barlow<sup>50</sup>, C. Barschel<sup>37</sup>, S. Barsuk<sup>7</sup>, A. Bates<sup>47</sup>, C. Bauer<sup>10</sup>, Th. Bauer<sup>23</sup>, A. Bay<sup>38</sup>, I. Bediaga<sup>1</sup>, K. Belous<sup>34</sup>, I. Belyaev<sup>30,37</sup>, E. Ben-Haim<sup>8</sup>, M. Benayoun<sup>8</sup>, G. Bencivenni<sup>18</sup>, R. Bernet<sup>39</sup>, M.-O. Bettler<sup>17,37</sup>, M. van Beuzekom<sup>23</sup>, S. Bifani<sup>12</sup>, A. Bizzeti<sup>17,h</sup>, P.M. Bjørnstad<sup>50</sup>, T. Blake<sup>49</sup>, F. Blanc<sup>38</sup>, C. Blanks<sup>49</sup>, J. Blouw<sup>11</sup>, S. Blusk<sup>52</sup>, A. Bobrov<sup>33</sup>, V. Bocci<sup>22</sup>, A. Bondar<sup>33</sup>, N. Bondar<sup>29,37</sup>, W. Bonivento<sup>15</sup>, S. Borghi<sup>47</sup>, A. Borgia<sup>52</sup>, E. Bos<sup>23</sup>, T.J.V. Bowcock<sup>48</sup>, C. Bozzi<sup>16</sup>, T. Brambach<sup>9</sup>, J. van den Brand<sup>24</sup>, J. Bressieux<sup>38</sup>, S. Brisbane<sup>51</sup>, M. Britsch<sup>10</sup>, T. Britton<sup>52</sup>, N.H. Brook<sup>42</sup>, H. Brown<sup>48</sup>, A. Büchler-Germann<sup>39</sup>, A. Bursche<sup>39</sup>, J. Buytaert<sup>37</sup>, S. Cadeddu<sup>15</sup>, J.M. Caicedo Carvajal<sup>37</sup>, O. Callot<sup>7</sup>, M. Calvi<sup>20,j</sup>, M. Calvo Gomez<sup>35,n</sup>, A. Camboni<sup>35</sup>, L. Camilleri<sup>37</sup>, P. Campana<sup>18</sup>, G. Capon<sup>18</sup>, A. Carbone<sup>14</sup>, G. Carboni<sup>21,k</sup>, R. Cardinale<sup>19,i</sup>, A. Cardini<sup>15</sup>, L. Carson<sup>36</sup>, K. Carvalho Akiba<sup>23</sup>, G. Casse<sup>48</sup>, M. Cattaneo<sup>37</sup>, M. Charles<sup>51</sup>, Ph. Charpentier<sup>37</sup>, N. Chiapolini<sup>39</sup>, X. Cid Vidal<sup>36</sup>, P.J. Clark<sup>46</sup>, P.E.L. Clarke<sup>46</sup>, M. Clemencic<sup>37</sup>, H.V. Cliff<sup>43</sup>, J. Closier<sup>37</sup>, C. Coca<sup>28</sup>, V. Coco<sup>23</sup>, J. Cogan<sup>6</sup>, P. Collins<sup>37</sup>, F. Constantin<sup>28</sup>, G. Conti<sup>38</sup>, A. Contu<sup>51</sup>, M. Coombes<sup>42</sup>, G. Corti<sup>37</sup>, G.A. Cowan<sup>38</sup>, R. Currie<sup>46</sup>, B. D'Almagne<sup>7</sup>, C. D'Ambrosio<sup>37</sup>, W. Da Silva<sup>8</sup>, P. David<sup>8</sup>, I. De Bonis<sup>4</sup>, S. De Capua<sup>21,k</sup>, M. De Cian<sup>39</sup>, F. De Lorenzi<sup>12</sup>, J.M. De Miranda<sup>1</sup>, L. De Paula<sup>2</sup>, P. De Simone<sup>18</sup>, D. Decamp<sup>4</sup>, H. Degaudenzi<sup>38,37</sup>, M. Deissenroth<sup>11</sup>, L. Del Buono<sup>8</sup>, C. Deplano<sup>15</sup>, O. Deschamps<sup>5</sup>, F. Dettori<sup>15,d</sup>, J. Dickens<sup>43</sup>,

H. Dijkstra<sup>37</sup>, M. Dima<sup>28</sup>, P. Diniz Batista<sup>1</sup>, S. Donleavy<sup>48</sup>, D. Dossett<sup>44</sup>, A. Dovbnya<sup>40</sup>, F. Dupertuis<sup>38</sup>, R. Dzhelyadin<sup>34</sup>, C. Eames<sup>49</sup>, S. Easo<sup>45</sup>, U. Egede<sup>49</sup>, V. Egorychev<sup>30</sup>, S. Eidelman<sup>33</sup>, D. van Eijk<sup>23</sup>, F. Eisele<sup>11</sup>, S. Eisenhardt<sup>46</sup>, L. Eklund<sup>47</sup>, D.G. d'Enterria<sup>35,o</sup>, D. Esperante Pereira<sup>36</sup>, L. Estève<sup>43</sup>, E. Fanchini<sup>20,j</sup>, C. Färber<sup>11</sup>, G. Fardell<sup>46</sup>, C. Farinelli<sup>23</sup>, S. Farry<sup>12</sup>, V. Fave<sup>38</sup>, V. Fernandez Albor<sup>36</sup>, M. Ferro-Luzzi<sup>37</sup>, S. Filippov<sup>32</sup>, C. Fitzpatrick<sup>46</sup>, F. Fontanelli<sup>19,i</sup>, R. Forty<sup>37</sup>, M. Frank<sup>37</sup>, C. Frei<sup>37</sup>, M. Frosini<sup>17,f</sup>, J.L. Fungueirino Pazos<sup>36</sup>, S. Furcas<sup>20</sup>, A. Gallas Torreira<sup>36</sup>, D. Galli<sup>14,c</sup>, M. Gandelman<sup>2</sup>, P. Gandini<sup>51</sup>, Y. Gao<sup>3</sup>, J.-C. Garnier<sup>37</sup>, J. Garofoli<sup>52</sup>, L. Garrido<sup>35</sup>, C. Gaspar<sup>37</sup>, N. Gauvin<sup>38</sup>, M. Gersabeck<sup>37</sup>, T. Gershon<sup>44</sup>, Ph. Ghez<sup>4</sup>, V. Gibson<sup>43</sup>, V.V. Gligorov<sup>37</sup>, C. Göbel<sup>54</sup>, D. Golubkov<sup>30</sup>, A. Golutvin<sup>49,30,37</sup>, A. Gomes<sup>2</sup>, H. Gordon<sup>51</sup>, M. Grabalosa Gándara<sup>35</sup>, R. Graciani Diaz<sup>35</sup>, L.A. Granado Cardoso<sup>37</sup>, E. Graugés<sup>35</sup>, G. Graziani<sup>17</sup>, A. Greco<sup>28</sup>, S. Gregson<sup>43</sup>, B. Gui<sup>52</sup>, E. Gushchin<sup>32</sup>, Yu. Guz<sup>34,37</sup>, T. Gys<sup>37</sup>, G. Haefeli<sup>38</sup>, S.C. Haines<sup>43</sup>, T. Hampson<sup>42</sup>, S. Hansmann-Menzemer<sup>11</sup>, R. Harji<sup>49</sup>, N. Harnew<sup>51</sup>, P.F. Harrison<sup>44</sup>, J. He<sup>7</sup>, K. Hennessy<sup>48</sup>, P. Henrard<sup>5</sup>, J.A. Hernando Morata<sup>36</sup>, E. van Herwijnen<sup>37</sup>, A. Hicheur<sup>38</sup>, E. Hicks<sup>48</sup>, W. Hofmann<sup>10</sup>, K. Holubyev<sup>11</sup>, P. Hopchev<sup>4</sup>, W. Hulsbergen<sup>23</sup>, P. Hunt<sup>51</sup>, T. Huse<sup>48</sup>, R.S. Huston<sup>12</sup>, D. Hutchcroft<sup>48</sup>, V. Iakovenko<sup>7,41</sup>, C. Iglesias Escudero<sup>36</sup>, P. Ilten<sup>12</sup>, J. Imong<sup>42</sup>, R. Jacobsson<sup>37</sup>, M. Jahjah Hussein<sup>5</sup>, E. Jans<sup>23</sup>, F. Jansen<sup>23</sup>, P. Jaton<sup>38</sup>, B. Jean-Marie<sup>7</sup>, F. Jing<sup>3</sup>, M. John<sup>51</sup>, D. Johnson<sup>51</sup>, C.R. Jones<sup>43</sup>, B. Jost<sup>37</sup>, F. Kapusta<sup>8</sup>, T.M. Karbach<sup>9</sup>, J. Keaveney<sup>12</sup>, U. Kerzel<sup>37</sup>, T. Ketel<sup>24</sup>, A. Keune<sup>38</sup>, B. Khanji<sup>6</sup>, Y.M. Kim<sup>46</sup>, M. Knecht<sup>38</sup>, S. Koblitz<sup>37</sup>, A. Konoplyannikov<sup>30</sup>, P. Koppenburg<sup>23</sup>, A. Kozlinskiy<sup>23</sup>, L. Kravchuk<sup>32</sup>, G. Krocker<sup>11</sup>, P. Krokovny<sup>11</sup>, F. Kruse<sup>9</sup>, K. Kruzelecki<sup>37</sup>, M. Kucharczyk<sup>25</sup>, S. Kukulak<sup>25</sup>, R. Kumar<sup>14,37</sup>, T. Kvaratskheliya<sup>30</sup>, V.N. La Thi<sup>38</sup>, D. Lacarrere<sup>37</sup>, G. Lafferty<sup>50</sup>, A. Lai<sup>15</sup>, R.W. Lambert<sup>37</sup>, G. Lanfranchi<sup>18</sup>, C. Langenbruch<sup>11</sup>, T. Latham<sup>44</sup>, R. Le Gac<sup>6</sup>, J. van Leerdam<sup>23</sup>, J.-P. Lees<sup>4</sup>, R. Lefèvre<sup>5</sup>, A. Leflat<sup>31,37</sup>, J. Lefrançois<sup>7</sup>, O. Leroy<sup>6</sup>, T. Lesiak<sup>25</sup>, L. Li<sup>3</sup>, Y.Y. Li<sup>43</sup>, L. Li Gioi<sup>5</sup>, M. Lieng<sup>9</sup>, M. Liles<sup>48</sup>, R. Lindner<sup>37</sup>, C. Linn<sup>11</sup>, B. Liu<sup>3</sup>, G. Liu<sup>37</sup>, J.H. Lopes<sup>2</sup>, E. Lopez Asamar<sup>35</sup>, N. Lopez-March<sup>38</sup>, J. Luisier<sup>38</sup>, B. M'charek<sup>24</sup>, F. Machefert<sup>7</sup>, I.V. Machikhiliyan<sup>4,30</sup>, F. Maciuc<sup>10</sup>, O. Maev<sup>29</sup>, J. Magnin<sup>1</sup>, A. Maier<sup>37</sup>, S. Malde<sup>51</sup>, R.M.D. Mamunur<sup>37</sup>, G. Manca<sup>15,37,d</sup>, G. Mancinelli<sup>6</sup>, N. Mangiafave<sup>43</sup>, U. Marconi<sup>14</sup>, R. Märki<sup>38</sup>, J. Marks<sup>11</sup>, G. Martellotti<sup>22</sup>, A. Martens<sup>7</sup>, L. Martin<sup>51</sup>, A. Martin Sanchez<sup>7</sup>, D. Martinez Santos<sup>37</sup>, A. Massafferri<sup>1</sup>, Z. Mathe<sup>12</sup>, C. Matteuzzi<sup>20</sup>, M. Matveev<sup>29</sup>, V. Matveev<sup>34</sup>, E. Maurice<sup>6</sup>, B. Maynard<sup>52</sup>, A. Mazurov<sup>32</sup>, G. McGregor<sup>50</sup>, R. McNulty<sup>12</sup>, C. Mclean<sup>46</sup>, M. Meissner<sup>11</sup>, M. Merk<sup>23</sup>, J. Merkel<sup>9</sup>, M. Merkin<sup>31</sup>, R. Messi<sup>21,k</sup>, S. Miglioranzi<sup>37</sup>, D.A. Milanes<sup>13</sup>, M.-N. Minard<sup>4</sup>, S. Monteil<sup>5</sup>, D. Moran<sup>12</sup>, P. Morawski<sup>25</sup>, J.V. Morris<sup>45</sup>, R. Mountain<sup>52</sup>, I. Mous<sup>23</sup>, F. Muheim<sup>46</sup>, K. Müller<sup>39</sup>, R. Muresan<sup>28,38</sup>, F. Murtas<sup>18</sup>, B. Muryn<sup>26</sup>, M. Musy<sup>35</sup>, J. Mylroie-Smith<sup>48</sup>, P. Naik<sup>42</sup>, T. Nakada<sup>38</sup>, R. Nandakumar<sup>45</sup>, J. Nardulli<sup>45</sup>, M. Nedos<sup>9</sup>, M. Needham<sup>46</sup>, N. Neufeld<sup>37</sup>, M. Nicol<sup>7</sup>, S. Nies<sup>9</sup>, V. Niess<sup>5</sup>, N. Nikitin<sup>31</sup>, A. Oblakowska-Mucha<sup>26</sup>, V. Obraztsov<sup>34</sup>, S. Oggero<sup>23</sup>, O. Okhrimenko<sup>41</sup>, R. Oldeman<sup>15,d</sup>, M. Orlandea<sup>28</sup>, A. Ostankov<sup>34</sup>, B. Pal<sup>52</sup>, J. Palacios<sup>39</sup>, M. Palutan<sup>18</sup>, J. Panman<sup>37</sup>, A. Papanestis<sup>45</sup>, M. Pappagallo<sup>13,b</sup>, C. Parkes<sup>47,37</sup>, C.J. Parkinson<sup>49</sup>, G. Passaleva<sup>17</sup>, G.D. Patel<sup>48</sup>, M. Patel<sup>49</sup>, S.K. Paterson<sup>49,37</sup>, G.N. Patrick<sup>45</sup>, C. Patrignani<sup>19,i</sup>, C. Pavel-Nicorescu<sup>28</sup>, A. Pazos Alvarez<sup>36</sup>, A. Pellegrino<sup>23</sup>, G. Penso<sup>22,l</sup>, M. Pepe Altarelli<sup>37</sup>, S. Perazzini<sup>14,c</sup>, D.L. Perego<sup>20,j</sup>, E. Perez Trigo<sup>36</sup>, A. Pérez-Calero Yzquierdo<sup>35</sup>, P. Perret<sup>5</sup>, A. Petrella<sup>16,37,e</sup>, A. Petrolini<sup>19,i</sup>, B. Pie Valls<sup>35</sup>, B. Pietrzyk<sup>4</sup>, D. Pinci<sup>22</sup>, R. Plackett<sup>47</sup>, S. Playfer<sup>46</sup>, M. Plo Casasus<sup>36</sup>, G. Polok<sup>25</sup>, A. Poluektov<sup>44,33</sup>, E. Polycarpo<sup>2</sup>, D. Popov<sup>10</sup>, B. Popovici<sup>28</sup>, C. Potterat<sup>38</sup>, A. Powell<sup>51</sup>, T. du Pree<sup>23</sup>, V. Pugatch<sup>41</sup>, A. Puig Navarro<sup>35</sup>, W. Qian<sup>3</sup>, J.H. Rademacker<sup>42</sup>, B. Rakotomiamanana<sup>38</sup>, I. Raniuk<sup>40</sup>, G. Raven<sup>24</sup>, S. Redford<sup>51</sup>, W. Reece<sup>49</sup>, A.C. dos Reis<sup>1</sup>, S. Ricciardi<sup>45</sup>, K. Rinnert<sup>48</sup>, D.A. Roa Romero<sup>5</sup>, P. Robbe<sup>7,37</sup>, E. Rodrigues<sup>47</sup>, F. Rodrigues<sup>2</sup>, C. Rodriguez Cobo<sup>36</sup>, P. Rodriguez Perez<sup>36</sup>, G.J. Rogers<sup>43</sup>, V. Romanovsky<sup>34</sup>, J. Rouvinet<sup>38</sup>, T. Ruf<sup>37</sup>, H. Ruiz<sup>35</sup>, G. Sabatino<sup>21,k</sup>, J.J. Saborido Silva<sup>36</sup>, N. Sagidova<sup>29</sup>, P. Sail<sup>47</sup>, B. Saitta<sup>15,d</sup>, C. Salzmann<sup>39</sup>, A. Sambade Varela<sup>37</sup>, M. Sannino<sup>19,i</sup>, R. Santacesaria<sup>22</sup>, R. Santinelli<sup>37</sup>, E. Santovetti<sup>21,k</sup>, M. Sapunov<sup>6</sup>, A. Sarti<sup>18</sup>, C. Satriano<sup>22,m</sup>, A. Satta<sup>21</sup>, M. Savrie<sup>16,e</sup>, D. Savrina<sup>30</sup>, P. Schaack<sup>49</sup>, M. Schiller<sup>11</sup>, S. Schleich<sup>9</sup>, M. Schmelling<sup>10</sup>, B. Schmidt<sup>37</sup>, O. Schneider<sup>38</sup>, A. Schopper<sup>37</sup>, M.-H. Schune<sup>7</sup>, R. Schwemmer<sup>37</sup>, A. Sciubba<sup>18,l</sup>, M. Seco<sup>36</sup>, A. Semennikov<sup>30</sup>, K. Senderowska<sup>26</sup>, N. Serra<sup>23</sup>, J. Serrano<sup>6</sup>, B. Shao<sup>3</sup>, M. Shapkin<sup>34</sup>, I. Shapoval<sup>40,37</sup>, P. Shatalov<sup>30</sup>, Y. Shcheglov<sup>29</sup>, T. Shears<sup>48</sup>, L. Shekhtman<sup>33</sup>, O. Shevchenko<sup>40</sup>, V. Shevchenko<sup>30</sup>, A. Shires<sup>49</sup>, E. Simioni<sup>24</sup>, H.P. Skottowe<sup>43</sup>, T. Skwarnicki<sup>52</sup>, A.C. Smith<sup>37</sup>, K. Sobczak<sup>5</sup>, F.J.P. Soler<sup>47</sup>, A. Solomin<sup>42</sup>, P. Somogy<sup>37</sup>, F. Soomro<sup>49</sup>, B. Souza De Paula<sup>2</sup>, B. Spaan<sup>9</sup>, A. Sparkes<sup>46</sup>, E. Spiridenkov<sup>29</sup>, P. Spradlin<sup>51</sup>,

F. Stagni<sup>37</sup>, O. Steinkamp<sup>39</sup>, O. Stenyakin<sup>34</sup>, S. Stoica<sup>28</sup>, S. Stone<sup>52,\*</sup>, B. Storaci<sup>23</sup>, U. Straumann<sup>39</sup>, N. Styles<sup>46</sup>, M. Szczekowski<sup>27</sup>, P. Szczypka<sup>38</sup>, T. Szumlak<sup>26</sup>, S. T'Jampens<sup>4</sup>, V. Talanov<sup>34</sup>, E. Teodorescu<sup>28</sup>, H. Terrier<sup>23</sup>, F. Teubert<sup>37</sup>, C. Thomas<sup>51,45</sup>, E. Thomas<sup>37</sup>, J. van Tilburg<sup>39</sup>, V. Tisserand<sup>4</sup>, M. Tobin<sup>39</sup>, S. Topp-Joergensen<sup>51</sup>, M.T. Tran<sup>38</sup>, A. Tsaregorodtsev<sup>6</sup>, N. Tuning<sup>23</sup>, A. Ukleja<sup>27</sup>, P. Urquijo<sup>52</sup>, U. Uwer<sup>11</sup>, V. Vagnoni<sup>14</sup>, G. Valenti<sup>14</sup>, R. Vazquez Gomez<sup>35</sup>, P. Vazquez Regueiro<sup>36</sup>, S. Vecchi<sup>16</sup>, J.J. Velthuis<sup>42</sup>, M. Veltri<sup>17,g</sup>, K. Vervink<sup>37</sup>, B. Viaud<sup>7</sup>, I. Videau<sup>7</sup>, X. Vilasis-Cardona<sup>35,n</sup>, J. Visniakov<sup>36</sup>, A. Vollhardt<sup>39</sup>, D. Voong<sup>42</sup>, A. Vorobyev<sup>29</sup>, An. Vorobyev<sup>29</sup>, H. Voss<sup>10</sup>, K. Wacker<sup>9</sup>, S. Wandernoth<sup>11</sup>, J. Wang<sup>52</sup>, D.R. Ward<sup>43</sup>, A.D. Webber<sup>50</sup>, D. Websdale<sup>49</sup>, M. Whitehead<sup>44</sup>, D. Wiedner<sup>11</sup>, L. Wiggers<sup>23</sup>, G. Wilkinson<sup>51</sup>, M.P. Williams<sup>44,45</sup>, M. Williams<sup>49</sup>, F.F. Wilson<sup>45</sup>, J. Wishahi<sup>9</sup>, M. Witek<sup>25</sup>, W. Witzeling<sup>37</sup>, S.A. Wotton<sup>43</sup>, K. Wyllie<sup>37</sup>, Y. Xie<sup>46</sup>, F. Xing<sup>51</sup>, Z. Yang<sup>3</sup>, G. Ybeles Smit<sup>23</sup>, R. Young<sup>46</sup>, O. Yushchenko<sup>34</sup>, M. Zavertyaev<sup>10,a</sup>, L. Zhang<sup>52</sup>, W.C. Zhang<sup>12</sup>, Y. Zhang<sup>3</sup>, A. Zhelezov<sup>11</sup>, L. Zhong<sup>3</sup>, E. Zverev<sup>31</sup>

<sup>1</sup> Centro Brasileiro de Pesquisas Físicas (CBPF), Rio de Janeiro, Brazil

<sup>2</sup> Universidade Federal do Rio de Janeiro (UFRJ), Rio de Janeiro, Brazil

<sup>3</sup> Center for High Energy Physics, Tsinghua University, Beijing, China

<sup>4</sup> LAPP, Université de Savoie, CNRS/IN2P3, Annecy-Le-Vieux, France

<sup>5</sup> Clermont Université, Université Blaise Pascal, CNRS/IN2P3, LPC, Clermont-Ferrand, France

<sup>6</sup> CPPM, Aix-Marseille Université, CNRS/IN2P3, Marseille, France

<sup>7</sup> LAL, Université Paris-Sud, CNRS/IN2P3, Orsay, France

<sup>8</sup> LPNHE, Université Pierre et Marie Curie, Université Paris Diderot, CNRS/IN2P3, Paris, France

<sup>9</sup> Fakultät Physik, Technische Universität Dortmund, Dortmund, Germany

<sup>10</sup> Max-Planck-Institut für Kernphysik (MPIK), Heidelberg, Germany

<sup>11</sup> Physikalisches Institut, Ruprecht-Karls-Universität Heidelberg, Heidelberg, Germany

<sup>12</sup> School of Physics, University College Dublin, Dublin, Ireland

<sup>13</sup> Sezione INFN di Bari, Bari, Italy

<sup>14</sup> Sezione INFN di Bologna, Bologna, Italy

<sup>15</sup> Sezione INFN di Cagliari, Cagliari, Italy

<sup>16</sup> Sezione INFN di Ferrara, Ferrara, Italy

<sup>17</sup> Sezione INFN di Firenze, Firenze, Italy

<sup>18</sup> Laboratori Nazionali dell'INFN di Frascati, Frascati, Italy

<sup>19</sup> Sezione INFN di Genova, Genova, Italy

<sup>20</sup> Sezione INFN di Milano Bicocca, Milano, Italy

<sup>21</sup> Sezione INFN di Roma Tor Vergata, Roma, Italy

<sup>22</sup> Sezione INFN di Roma Sapienza, Roma, Italy

<sup>23</sup> Nikhef National Institute for Subatomic Physics, Amsterdam, Netherlands

<sup>24</sup> Nikhef National Institute for Subatomic Physics and Vrije Universiteit, Amsterdam, Netherlands

<sup>25</sup> Henryk Niewodniczanski Institute of Nuclear Physics Polish Academy of Sciences, Cracow, Poland

<sup>26</sup> Faculty of Physics & Applied Computer Science, Cracow, Poland

<sup>27</sup> Soltan Institute for Nuclear Studies, Warsaw, Poland

<sup>28</sup> Horia Hulubei National Institute of Physics and Nuclear Engineering, Bucharest-Magurele, Romania

<sup>29</sup> Petersburg Nuclear Physics Institute (PNPI), Gatchina, Russia

<sup>30</sup> Institute of Theoretical and Experimental Physics (ITEP), Moscow, Russia

<sup>31</sup> Institute of Nuclear Physics, Moscow State University (SINP MSU), Moscow, Russia

<sup>32</sup> Institute for Nuclear Research of the Russian Academy of Sciences (INR RAN), Moscow, Russia

<sup>33</sup> Budker Institute of Nuclear Physics (BINP), Novosibirsk, Russia

<sup>34</sup> Institute for High Energy Physics (IHEP), Protvino, Russia

<sup>35</sup> Universitat de Barcelona, Barcelona, Spain

<sup>36</sup> Universidad de Santiago de Compostela, Santiago de Compostela, Spain

<sup>37</sup> European Organization for Nuclear Research (CERN), Geneva, Switzerland

<sup>38</sup> Ecole Polytechnique Fédérale de Lausanne (EPFL), Lausanne, Switzerland

<sup>39</sup> Physik-Institut, Universität Zürich, Zürich, Switzerland

<sup>40</sup> NSC Kharkiv Institute of Physics and Technology (NSC KIPT), Kharkiv, Ukraine

<sup>41</sup> Institute for Nuclear Research of the National Academy of Sciences (KINR), Kyiv, Ukraine

<sup>42</sup> H.H. Wills Physics Laboratory, University of Bristol, Bristol, United Kingdom

<sup>43</sup> Cavendish Laboratory, University of Cambridge, Cambridge, United Kingdom

<sup>44</sup> Department of Physics, University of Warwick, Coventry, United Kingdom

<sup>45</sup> STFC Rutherford Appleton Laboratory, Didcot, United Kingdom

<sup>46</sup> School of Physics and Astronomy, University of Edinburgh, Edinburgh, United Kingdom

<sup>47</sup> School of Physics and Astronomy, University of Glasgow, Glasgow, United Kingdom

<sup>48</sup> Oliver Lodge Laboratory, University of Liverpool, Liverpool, United Kingdom

<sup>49</sup> Imperial College London, London, United Kingdom

<sup>50</sup> School of Physics and Astronomy, University of Manchester, Manchester, United Kingdom

<sup>51</sup> Department of Physics, University of Oxford, Oxford, United Kingdom

<sup>52</sup> Syracuse University, Syracuse, NY, United States

<sup>53</sup> CC-IN2P3, CNRS/IN2P3, Lyon-Villeurbanne, France<sup>P</sup>

<sup>54</sup> Pontifícia Universidade Católica do Rio de Janeiro (PUC-Rio), Rio de Janeiro, Brazil<sup>Q</sup>

\* Corresponding author.

E-mail address: stone@physics.syr.edu (S. Stone).

<sup>a</sup> P.N. Lebedev Physical Institute, Russian Academy of Science (LPI RAS), Moscow, Russia.

<sup>b</sup> Università di Bari, Bari, Italy.



- <sup>c</sup> Università di Bologna, Bologna, Italy.
- <sup>d</sup> Università di Cagliari, Cagliari, Italy.
- <sup>e</sup> Università di Ferrara, Ferrara, Italy.
- <sup>f</sup> Università di Firenze, Firenze, Italy.
- <sup>g</sup> Università di Urbino, Urbino, Italy.
- <sup>h</sup> Università di Modena e Reggio Emilia, Modena, Italy.
- <sup>i</sup> Università di Genova, Genova, Italy.
- <sup>j</sup> Università di Milano Bicocca, Milano, Italy.
- <sup>k</sup> Università di Roma Tor Vergata, Roma, Italy.
- <sup>l</sup> Università di Roma La Sapienza, Roma, Italy.
- <sup>m</sup> Università della Basilicata, Potenza, Italy.
- <sup>n</sup> LIFAELS, La Salle, Universitat Ramon Llull, Barcelona, Spain.
- <sup>o</sup> Institució Catalana de Recerca i Estudis Avançats (ICREA), Barcelona, Spain.
- <sup>p</sup> Associated member.
- <sup>q</sup> Associated to Universidade Federal do Rio de Janeiro (UFRJ), Rio de Janeiro, Brazil.